Spin dynamics in two-dimensional electron and hole systems revealed by resonant spin amplification

T. Korn[a], M. Griesbeck[a], M. Kugler[a], S. Furthmeier[a], C. Gradl[a], M. Hirmer[a], D. Schuh[a], W. Wegscheider[b], K. Korzekwa[c], P. Machnikowski[c], T. Kuhn[d], M.M. Glazov[e], E.Ya. Sherman[f,g], C. Schüller[a]

[a]Institut für Experimentelle und Angewandte Physik, Universität Regensburg, D-93040 Regensburg, Germany
[b]Solid State Physics Laboratory, ETH Zurich, 8093 Zurich, Switzerland
[c]Institute of Physics, Wrocław University of Technology, 50-370 Wrocław, Poland
[d]Institut für Festkörpertheorie, Westfälische Wilhelms-Universität, D-48149 Münster, Germany
[e]Ioffe Physical-Technical Institute, Russian Academy of Sciences, 194021 St. Petersburg, Russia
[f]Department of Physical Chemistry, The University of the Basque Country UPV/EHU, 48080 Bilbao, Spain
[g]IKERBASQUE Basque Foundation for Science, 48011 Bilbao, Bizkaia, Spain

ABSTRACT

Understanding and controlling the spin dynamics in semiconductor heterostructures is a key requirement for the design of future spintronics devices. In GaAs-based heterostructures, electrons and holes have very different spin dynamics. Some control over the spin-orbit fields, which drive the electron spin dynamics, is possible by choosing the crystallographic growth axis. Here, (110)-grown structures are interesting, as the Dresselhaus spin-orbit fields are oriented along the growth axis and therefore, the typically dominant Dyakonov-Perel mechanism is suppressed for spins oriented along this axis, leading to long spin depasing times. By contrast, hole spin dephasing is typically very rapid due to the strong spin-orbit interaction of the p-like valence band states. For localized holes, however, most spin dephasing mechanisms are suppressed, and long spin dephasing times may be observed. Here, we present a study of electron and hole spin dynamics in GaAs-AlGaAs-based quantum wells. We apply the resonant spin amplification (RSA) technique, which allows us to extract all relevant spin dynamics parameters, such as g factors and dephasing times with high accuracy. A comparison of the measured RSA traces with the developed theory reveals the anisotropy of the spin dephasing in the (110)-grown two-dimensional electron systems, as well as the complex interplay between electron and hole spin and carrier dynamics in the two-dimensional hole systems.

Keywords: Spin dynamics, two-dimensional electron system, two-dimensional hole system, time-resolved spectroscopy

1. INTRODUCTION

Semiconductor spintronics[1–5] is a very active research field in solid-state physics. In this field, the direct-gap semiconductor GaAs, and heterostructures based on the GaAs/AlGaAs material system, is an especially attractive model system for a number of reasons. On the one hand, molecular beam epitaxy (MBE) of GaAs is well-established, allowing for the fabrication of high-mobility electron and hole systems grown along different crystallographic axes. On the other hand, pulsed laser systems for resonant excitation of these structures are readily available. Additionally, the optical selection rules allow for all-optical creation and detection of a spin polarization in GaAs-based heterostructures. Most of the experimental work in the past has been focussed on

Further author information: (Send correspondence to T.Korn)
E-mail: Tobias.korn@ur.de , Telephone: +49 / (0)941 / 943 -2055

Spintronics V, edited by Henri-Jean Drouhin, Jean-Eric Wegrowe, Manijeh Razeghi,
Proc. of SPIE Vol. 8461, 84610O · © 2012 SPIE · CCC code: 0277-786/12/$18 · doi: 10.1117/12.930840

n-doped GaAs bulk material,[6–10] quantum wells[11] and two-dimensional electron systems (2DES).[12,13] For 2DES grown along the [110] crystallographic direction, spin dephasing via the Dyakonov-Perel (DP) mechanism[14] is strongly suppressed for growth-axis-oriented spins,[15,16] while it remains active for other spin orientations.[17] By comparison, hole spin dynamics have been investigated with less intensity, in part due to the short hole spin dephasing times observed in bulk GaAs,[18] which stem from the strong spin-orbit interaction (SOI) and the degeneracy of light- and heavy-hole valence bands in the bulk. More recently, significantly longer hole spin dephasing times (SDT) have been observed for optically oriented holes in n-doped QWs,[19,20] in p-doped QW systems in which localization of holes occurs at low temperatures,[21–25] and also in quantum dots.[26]

Here, we present a study of spin dynamics in 2DHS and (110)-grown 2DES using, both, time-resolved Faraday/Kerr rotation techniques (TRFR/TRKR)[27] and the related resonant spin amplification technique,[6] which has previously been applied by a number of groups to different systems ranging from bulk GaAs to ensembles of doped quantum dots.[7,23,28,29] In 2DHS, we study the initialization process for transfer of spin polarization from optically oriented carriers to resident holes, as well as the temperature and magnetic-field dependence of the hole SDT. We observe hole SDTs in excess of 80 ns for low temperatures and small magnetic fields. In our (110)-grown 2DES, we observe a strong orientational anisotropy of the SDT, as well as a pronounced maximum of the out-of-plane SDT with temperature, which is related to the complex growth structure of the sample.

2. SAMPLE STRUCTURE AND EXPERIMENT

All our samples are grown by molecular beam epitaxy. The two-dimensional hole system sample contains a single-side p-modulation-doped GaAs/$Al_{0.3}Ga_{0.7}As$ QW (QW width 4 nm) with a hole density $p = 1.1 \times 10^{11}$ cm^{-2} and mobility $\mu = 1.3 \times 10^4$ cm^2/Vs measured at 1.3 K. Some samples from this wafer are thinned for measurements in transmission. For this, the samples are first glued onto a sapphire substrate with optically transparent glue, then the semiconductor substrate is removed by grinding and selective wet etching. The samples contain a short-period GaAs/AlGaAs superlattice, which serves as an etch stop, leaving only the MBE-grown layers.

The two-dimensional electron system sample contains a symmetrically n-modulation-doped, 30 nm wide GaAs QW in which the 2DES resides. It is similar in design to structures introduced by Umansky *et al.*[30] A total of four n-doping layers are deposited in the barrier material below and above the GaAs QW. While the doping layers far below and above the QW mostly serve to give flat-band conditions, the two closer doping layers provide the charge carriers for the 2DES. These doping layers are embedded between two 2 nm thick layers of AlAs, so that some of the dopant electrons occupy the X valley states in the AlAs layers and lead to partial screening of the dopant disorder potential.[31] This complex growth structure leads to a well-defined symmetric confinement of the 2DES in the QW, provided that the remote dopants are ionized. The nominal carrier density $n = 2.7 \times 10^{11}$ cm^{-2} and mobility $\mu = 2.3 \times 10^6$ cm^2(Vs)$^{-1}$ of the 2DES sample were determined at 1.5 K using magnetotransport. In similar structures grown on (001) substrates, even higher carrier mobilities above 18×10^6 cm^2(Vs)$^{-1}$ were observed at low temperatures, allowing us to study the spin dynamics of electrons on ballistic cyclotron orbits.[24,32]

Some of the RSA and TRKR/TRFR measurements are performed in an optical cryostat with ^{3}He insert, allowing us to lower the sample temperatures below 400 mK and to apply magnetic fields of up to 11.5 Tesla. Here, the samples are cooled by cold ^{3}He gas. For some of these measurements, thinned samples are used and the experiment is performed in transmission (Faraday rotation) to limit the amount of absorbed laser power. RSA and TRKR measurements at higher temperatures are performed in a Helium flow cryostat, in which the samples are mounted on the cold finger of the cryostat in vacuum. A room-temperature electromagnet is used to create in-plane magnetic fields of up to 0.4 Tesla.

A pulsed Ti-Sapphire laser system generating pulses with a length between 600 fs and 2 ps, and a corresponding spectral width of 1-4 meV, is used for the optical measurements. The repetition rate of the laser system is 80 MHz, corresponding to a time delay of 12.5 ns between subsequent pulses. The laser pulses are split into a circularly-polarized pump beam and a linearly-polarized probe beam by a beam splitter. A mechanical delay line is used to create a variable time delay between pump and probe. The length of this delay line limits the observable time window in TRKR measurements to about 2 ns. Both beams are focussed to a diameter of about 80 μm on the sample using an achromat. For some measurements on the 2DES sample, an additional, weak

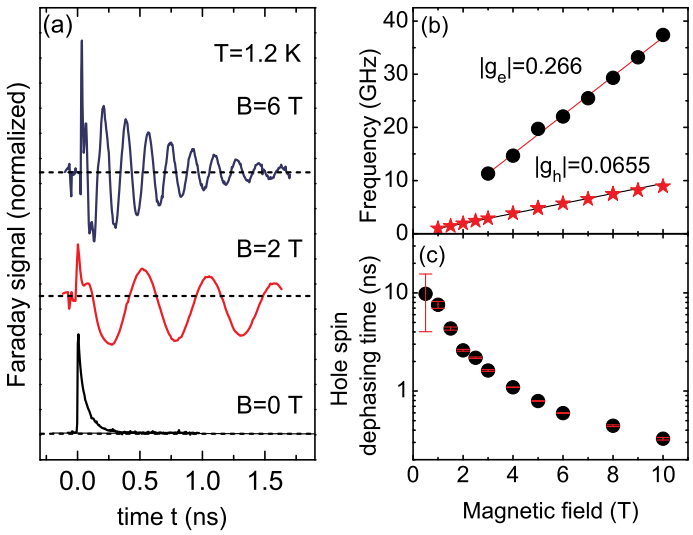

Figure 1. (a) Normalized time-resolved Faraday rotation traces measured on the 2DHS sample at 1.2 K with and without applied in-plane magnetic fields. (b) Electron and hole spin precession frequencies as a function of the applied in-plane magnetic field. (c) Hole spin dephasing time as a function of the applied in-plane magnetic field.

above-barrier illumination with a 532 nm continuous-wave laser is used. This laser is focussed to a large spot diameter overlapping the laser spot used in TRKR.

In the TRKR and RSA experiments, the circularly-polarized pump beam is generating electron-hole pairs in the QW, with spins aligned parallel or antiparallel to the beam direction, i.e., the QW normal, depending on the helicity of the light. In the TRKR measurements, the spin polarization created perpendicular to the sample plane by the pump beam, is probed by the time-delayed probe beam via the Kerr effect: the axis of linear polarization of the probe beam is rotated by a small angle, which is proportional to the out-of-plane component of the spin polarization.[33,34] This small angle is detected using an optical bridge. A lock-in scheme is used to increase sensitivity. The RSA technique is based on the interference of spin polarizations created in a sample by subsequent pump pulses. It requires that the spin dephasing time is comparable to the time delay between pump pulses. For certain magnetic fields applied in the sample plane, the optically oriented spin polarization precesses by an integer multiple of 2π in the time window between subsequent pump pulses, so that constructive interference occurs. This leads to pronounced maxima in the Faraday or Kerr rotation angle measured for a fixed time delay as a function of the applied magnetic field. In our measurements, the time delay is chosen to probe the spin polarization remaining within the sample 100 ps before the arrival of a pump pulse.

For initial characterization of the samples, PL measurements using continuous-wave excitation with a 532 nm laser or a Ti-Sapphire laser tuned to 780 nm are performed. A grating spectrometer with a Peltier-cooled charge coupled device (CCD) detector is used to collect the PL.

3. HOLE SPIN DYNAMICS IN A TWO-DIMENSIONAL HOLE SYSTEM

3.1 Time-resolved Faraday rotation

First, we study the spin dynamics in our 2DHS under resonant excitation using time-resolved Faraday rotation. Figure 1(a) shows typical Faraday traces measured with the sample at 1.2 K in different applied in-plane magnetic fields. We note that the zero-field Faraday rotation measurement shows only a simple exponential decay with a decay constant $\tau_r = 65$ ps. By contrast, the measurements in applied magnetic fields show long-lived precessional dynamics. This difference stems from the complex initialization process of the hole spin polarization, which will be discussed in more detail below. In the finite-field measurements, we observe two distinctly different precession frequencies, a fast precession, which decays rapidly, and a longer-lived, slow precession. For further analysis, the sum of two damped cosine functions with different amplitudes, decay constants and frequencies is fitted to the

TRFR traces. We identify the fast precession as the electron spin precession in the applied magnetic field, the g factor extracted from the magnetic field dependence of the precession frequency (Figure 1(b)), $|g_e| = 0.266$, is in good agreement with values expected for our QW width.[35] Since our samples are p-doped, the electron spin precession can only persist during the photocarrier lifetime. The slower, long-lived precession signal is due to hole spin precession and allows us to extract, both, the hole g factor, $|g_h| = 0.0655$, and the hole spin dephasing time, shown in Figure 1(c). We note that the hole SDT decreases with the applied magnetic field. This is due to inhomogeneous broadening: in our experiments, we study the hole spin dynamics of an ensemble of holes which are localized, e.g., at QW thickness fluctuations, and thus sample slightly different crystal environments. This leads to a spread Δg_h of the hole g factors. In an applied magnetic field, the hole ensemble will precess at different frequencies, so that the spin ensemble dephases. The ensemble spin dephasing time, T_2^*, is in first approximation given by[36]

$$T_2^* = \left(\frac{1}{T_2} + \frac{\Delta g_h \mu_B B}{\hbar} \right)^{-1}. \quad (1)$$

Here, T_2 is the SDT in absence of inhomogeneous broadening. In the TRFR measurements, a sufficiently large in-plane magnetic field has to be applied to the sample, so that at least one precessional cycle of the hole spin precession can be observed in the available time window of less than 2 ns. In this magnetic field range, the inhomogeneous broadening already limits the SDT, and the small time window leads to a large error of the damped cosine fit. It follows that in order to extract the T_2 time, measurements have to be performed in zero or low applied magnetic fields so that the inhomogeneous broadening is suppressed. Additionally, the determination of long spin dephasing times should not be limited by the accessible time window. These requirements are met in the RSA measurements discussed below.

3.2 Resonant spin amplification

We now turn to the discussion of resonant spin amplification measurements in our 2DHS. Figure 2(a) shows two RSA traces measured at 4.5 K and 0.4 K. We note that, in both traces, there is no RSA maximum at zero magnetic field. With increasing magnetic field, distinct, equidistant RSA peaks appear and their amplitude first increases, up to a magnetic field strength of about 400 mT, then decreases again. For the 0.4 K trace, RSA peaks can be detected up to about 2 Tesla. The trace measured at 4.5 K shows a significantly weaker signal and has been multiplied by a factor of 20 in Figure 2(a) for easier comparison. In order to understand the peculiar, butterfly-like shape of the RSA traces, we need to discuss the interplay between electron and hole spin and carrier dynamics in our sample, which was first discussed by Syperek et al.[21] By resonant optical excitation with circularly polarized light, we generate electron-hole pairs with their spin oriented along the growth direction. During the photocarrier recombination time, neither the electron nor the hole spin polarization dephases. Therefore, spin-polarized electrons will predominantly recombine with holes with matching spin orientation, leading to circularly polarized photoluminescence, and also to a removal of the spin polarization within the sample during the photocarrier lifetime. This process is sketched in the left panel of Figure 3(a). By applying a sufficiently large in-plane magnetic field, the electron and hole spins are forced to precess with different precession frequencies due to the large difference of their g factors. Therefore, during the photocarrier lifetime, electrons may recombine with resident holes with arbitrary spin orientation, leading to a transfer of spin polarization from the optically oriented holes to the resident 2DHS. This process is depicted in the right panel of Figure 3(a). This initialization process also explains why the zero-field TRFR trace in Figure 1(a) shows no long-lived hole spin signal. Correspondingly, in the RSA measurements, where the spin polarization of the resident carriers is measured at time delays which exceed the photocarrier recombination time, there is no zero-field signal. In small magnetic fields, a partial transfer of spin polarization to the resident holes takes place, allowing for constructive interference of spin polarizations from subsequent pump pulses, leading to the first maxima. As the magnetic field is increased further, the transfer process saturates, leading to pronounced RSA peaks. For higher magnetic fields, the inhomogeneous broadening leads to a reduction of the ensemble hole SDT, reducing the amplitude of the high-field RSA peaks. In order to model the combined spin and carrier dynamics, we used a set of coupled rate equations (not shown) for the electron and hole spin population,[23,24] similar to an approach used by Yugova et al.[34] to describe the initialization of a resident *electron* spin polarisation in n-doped QWs. This allows us to model the RSA traces in great detail, as shown in Figure 2(b) for a direct comparison between measured data (open circles) and simulated trace (solid line). Most of the parameters for the simulation, including electron

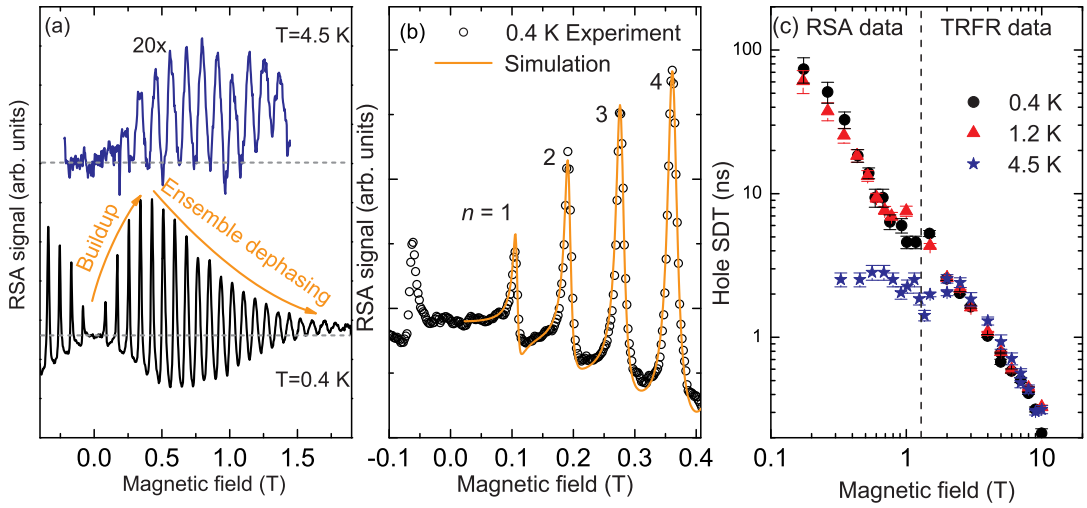

Figure 2. (a) RSA traces measured on the 2DHS sample at 4.5 K and 0.4 K. The 4.5 K data has been multiplied by a factor of 20 for easy comparison to the 0.4 K data. The orange arrows indicate different magnetic field regimes in the measurement. (b) RSA trace measured at 0.4 K compared to simulation. (c) Hole SDT T_2^* extracted from RSA traces (left part) and TRFR traces (right part) as a function of magnetic field for different temperatures.

and hole g factors, as well as the photocarrier recombination time, can be directly extracted from the TRFR measurements. By fitting the simulation to the measured RSA spectra, we can extract, in addition, the ensemble spin dephasing time as a function of the applied in-plane magnetic field. The results are given in Figure 2(c). Here, we combine the SDTs extracted from the RSA spectra (low-field region) with those extracted from TRFR (high-field region), for the three different measurement temperatures. We clearly see that for measurements at 0.4 K and 1.2 K, the hole SDT, T_2^*, increases as the magnetic field is reduced, reaching values well above 70 ns for the lowest fields in which we can obtain RSA maxima, while at 4.5 K, the SDT saturates at about 2.5 ns. In the high-field region, where TRFR measurements yield values for the hole SDT, the values for the three temperatures almost match, indicating that the inhomogeneous broadening masks any differences in the hole spin dynamics. Given the large values of the hole SDT, we need to discuss the possible hole spin dephasing mechanisms which provide a limitation for T_2 in the absence of inhomogeneous broadening. We can exclude that holes are thermally activated from their localization centers, which are formed by monolayer fluctuations of the QW thickness.[37] For a 4 nm wide QW, the localization energy exceeds 10 meV, which greatly exceeds the thermal energy even for the highest measurement temperature (E_{th}(4.5 K)=0.39 meV). While the contact hyperfine interaction of holes with nuclei is suppressed due to the p-like nature of the hole wave function, dipolar interaction between hole spins and nuclear spins is still possible.[38–40] The nuclei act as slowly varying random magnetic fields, which lead to both, single spin decoherence and ensemble spin dephasing. However, the effective nuclear magnetic fields can be efficiently suppressed by small in-plane magnetic fields, which we apply during the RSA measurements.[38] The dephasing process that is most likely to limit the hole SDT arises from the fact the even close to $k = 0$, there is a finite admixture of light-hole states to the heavy-hole state. In thin QWs, this admixture is on the order of 2 percent. Therefore, any momentum scattering may, with a finite probability, flip the hole spin, leading to spin dephasing. The spin dephasing rate is directly proportional to the momentum scattering rate, which in turn increases with the sample temperature. This mechanism also explains the drastic decrease of the small-field spin dephasing times with increasing temperature.

Finally, we discuss an alternative initialization mechanism for creating a resident hole spin polarization: under resonant excitation conditions, both, electrons and holes retain their spin orientation during the photocarrier lifetime. This makes it necessary to apply an in-plane magnetic field to induce spin precession, which in turn allows for a transfer of spin polarization to resident holes. By exciting our sample nonresonantly, we can create a different situation. If the pump laser is detuned to excite electron-hole pairs with a few meV of excess

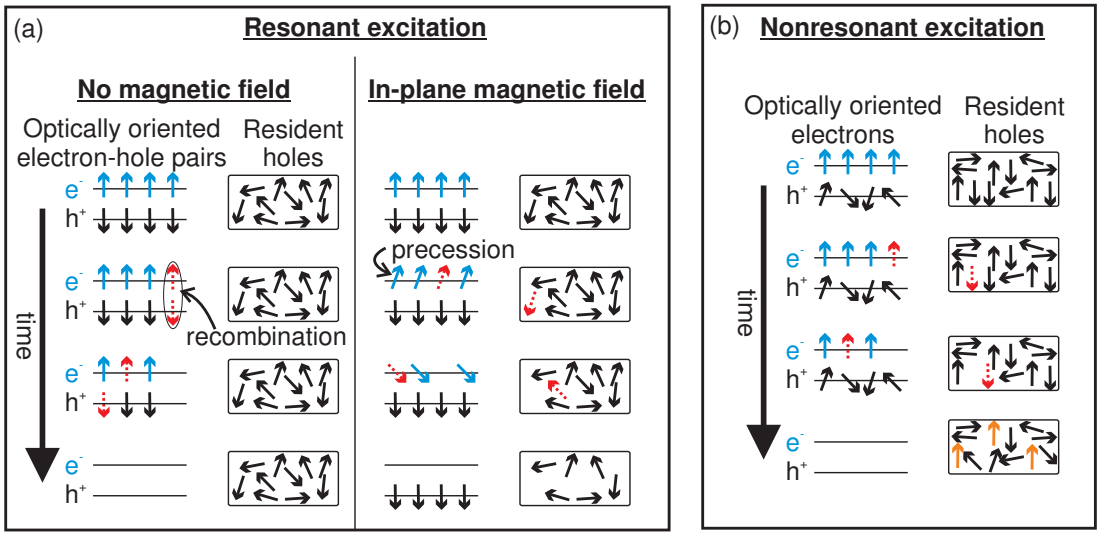

Figure 3. (a) Initialization of a hole spin polarization under resonant excitation conditions. Spin orientation of holes and electrons is indicated by the arrow direction. Electron-hole pairs that recombine are highlighted by red dashed arrows. (b) Initialization of a hole spin polarization under nonresonant excitation. Excess hole spin polarization in the resident hole ensemble is highlighted by orange arrows.

energy, both, electrons and holes relax to the band extrema within a few picoseconds. For electrons, this energy relaxation is typically spin-conserving. By contrast, holes typically lose their spin orientation during momentum and energy relaxation due to the mixed light-hole/heavy-hole character of the valence bands for $k > 0$. Correspondingly, after energy relaxation, the optically oriented holes are unpolarized. This situation is sketched in Figure 3(b). During photocarrier recombination, electrons will recombine with (resident) holes with matching spin orientation. This leads to an excess of resident holes with the *opposite* spin orientation. In this way, spin polarization is transferred from the optically oriented electrons to the 2DHS. We can directly observe this initialization mechanism in RSA spectra, as Figure 4 demonstrates. While RSA traces measured under weak, resonant excitation (black traces in both panels of Figure 4) have the previously discussed butterfly-like shape with no RSA peaks at zero magnetic field, the RSA trace shape changes drastically for nonresonant excitation (Figure 4 (a)) or high-intensity resonant excitation (Figure 4 (b)). Under these conditions, we observe RSA peaks at and around zero magnetic field pointing into the *opposite* direction compared to the resonant excitation peaks. For higher magnetic fields, even under nonresonant excitation conditions, we observe a sign change of the RSA peak orientation. We may explain these observations as follows: in zero and small applied magnetic fields, the transfer of spin polarization from optically oriented holes to resident holes is suppressed, as discussed above. However, resident holes may be initialized due to the recombination of spin-polarized electrons. The resulting hole spin polarization has the opposite sign, leading to an opposite sign of the Faraday or Kerr signal. The constructive interference of hole spin polarizations generated in this way leads to the observed RSA peaks at and around zero magnetic field. For intermediate fields, the precession-induced initialization process is activated and becomes dominant, leading to the sign reversal of the RSA peaks. From the shape of the RSA traces we may therefore infer that even under nonresonant or high-intensity excitation conditions, a part of the optically oriented holes retain their spin polarization during energy relaxation. In fact, we are able to quantify the hole spin polarization immediately after energy relaxation by modelling the spin and carrier dynamics[41] (not shown). Remarkably, the observation of RSA peaks with opposite sign also indicates that rapid hole spin relaxation and very long hole spin dephasing times *coexist* in our sample.

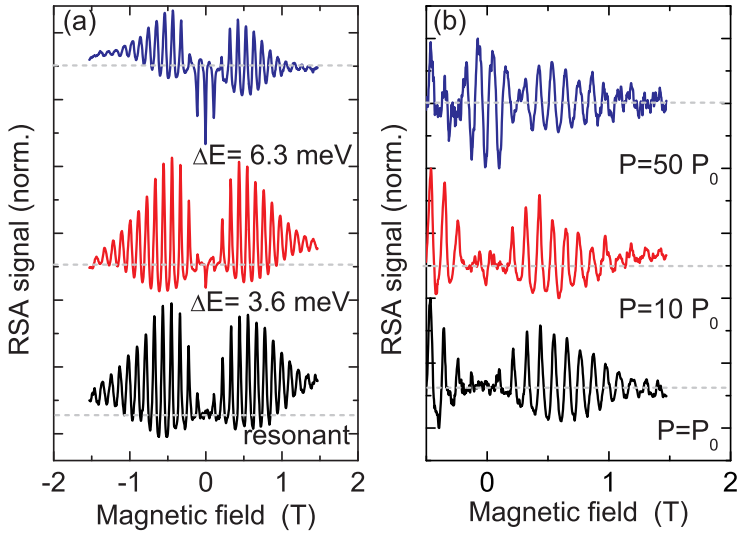

Figure 4. (a) RSA traces measured on the 2DHS sample at 1.2 K for resonant and nonresonant excitation. (b) RSA traces measured on the 2DHS sample at 1.2 K under resonant excitation for various excitation densities.

4. ELECTRON SPIN DYNAMICS IN A (110)-GROWN TWO-DIMENSIONAL ELECTRON SYSTEM

4.1 Time-resolved Kerr rotation

We now turn to the electron spin dynamics in our high-mobility, (110)-grown 2DES. First, we discuss the time-resolved Kerr rotation data. Figure 5 shows two Kerr rotation traces measured at 26 K with and without applied magnetic fields. The figure represents the raw data, i.e., the two traces have not been shifted vertically. We note that the zero-field measurement shows a step-like increase of the Kerr signal after the arrival of the pump pulse at $t = 0$. No decay of the spin polarization is observable within the time window available for the TRKR measurement. This indicates that, in contrast to the 2DHS system, the transfer of spin polarization from the optically oriented to the resident electrons is possible also at zero magnetic field and under resonant excitation conditions. This is due to the fact that the hole spin dephasing time in the 2DES is significantly shorter than the photocarrier lifetime, so that the optically created holes can recombine with electrons of arbitrary spin orientation. In the trace measured with an in-plane magnetic field, we observe pronounced spin precession, as well as a partial decay of the TRKR signal within the measurement window. Additionally, we note that the signal level at negative delay times is very different for the zero- and finite-field measurements, indicating that a constructive interference between spin polarizations created by subsequent pulses occurs at zero magnetic field. In fact, this constructive interference yields a larger Kerr signal than the spin polarization created by a single pulse. At the finite magnetic field shown in Figure 5, the spin precession rate is incommensurable to the pulse repetition rate of the laser, so that there is no constructive interference. The partial decay of the spin polarization in case of spin precession is expected due to the symmetry of the spin-orbit fields: in our symmetrically doped sample, the main contribution to the SOI stems from the Dresselhaus field, which is aligned along the growth direction for (110)-grown QWs. Hence, for spins not oriented along the growth direction, Dyakonov-Perel-like spin dephasing in the Dresselhaus field occurs. Our TRKR measurements clearly demonstrate the limitations of the technique in case of long spin dephasing times. We can extract qualitative information on the spin dynamics, e.g., an anisotropy of the spin dephasing for in- and out-of-plane spin orientation, but no quantitative analysis of the SDTs is possible due to the finite time window available for observation.

4.2 Resonant spin amplification

Next, we discuss resonant spin amplification measurements on the 2DES sample, which overcome the limitations of the TRKR measurements presented above. Figure 6(a) shows the typical shape of an RSA trace measured on the 2DES sample. We clearly see a pronounced maximum at zero magnetic field, which has a significantly

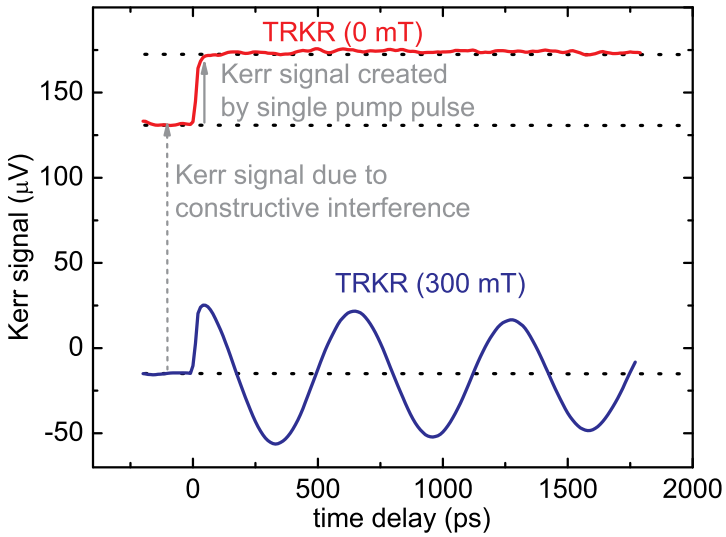

Figure 5. Time-resolved Kerr rotation traces measured on the 2DES sample at 26 K with and without applied in-plane magnetic fields. The curves have not been shifted vertically and allow for direct comparison of the Kerr signals before the arrival of a pump pulse.

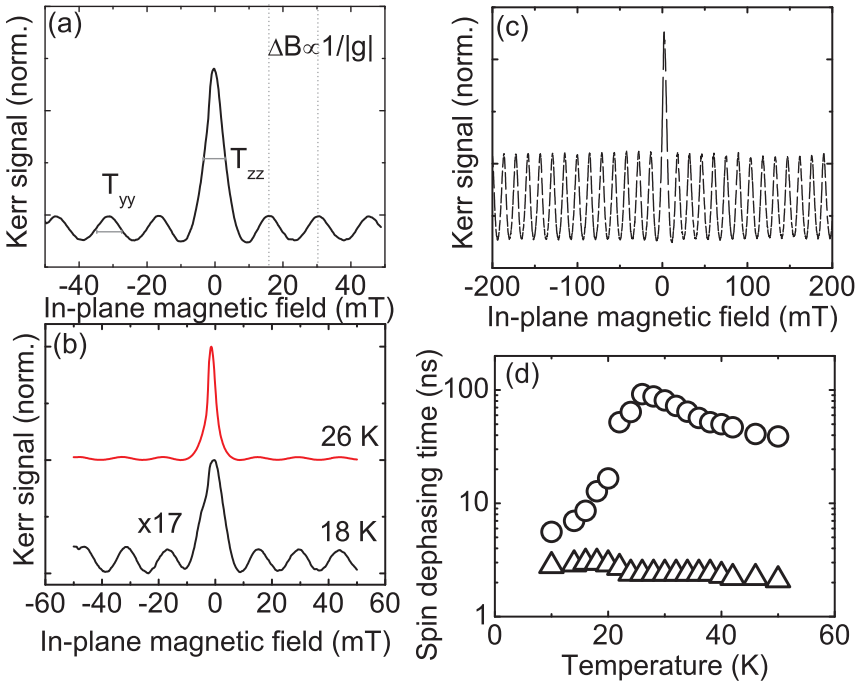

Figure 6. (a) Typical shape of the RSA trace measured on our 2DES sample. (b) RSA traces measured on the 2DES sample at two different temperatures. The trace measured at 18 K has been multiplied by a factor of 17 for easy comparison with the 26 K trace. (c) RSA trace measured at 4.5 K under weak, above-barrier illumination. (d) Temperature dependence of the out-of plane (open circles) and in-plane (open triangles) spin dephasing times in the 2DES sample.

larger amplitude than the surrounding maxima at finite fields. These additional maxima do not show a decay with increasing field amplitude, but remain at constant height. The shape of the RSA trace directly reflects the spin dynamics in the 2DES: for zero magnetic field, the DP mechanism is suppressed, resulting in a long spin dephasing time for out-of-plane oriented spins T_{zz}. Correspondingly, we observe a pronounced RSA peak with a small full width at half maximum (FWHM). For finite fields, DP-type spin dephasing in the Dresselhaus field occurs due to spin precession, leading to a smaller spin dephasing time for in-plane-oriented spins T_{yy}. Accordingly, we observe for finite-field RSA peaks a reduced amplitude and an increased FWHM. The fact that the amplitude of the finite-field RSA peaks remains constant within the magnetic field range investigated (see also Fig. 6(c), which shows an RSA trace measured with a larger field window) indicates that there is no significant g factor inhomogeneity in the 2DES. This is expected for free electrons: since the carriers are not localized, any inhomogeneities in the local g factor are averaged out due to the electron motion during the spin precession. In order to extract quantitative data from the RSA traces, we have developed an analytical expression for the RSA signal (not shown), taking into account the spin dephasing anisotropy.[42–44] By fitting this expression to the traces, we are able to extract all relevant parameters, including T_{zz}, T_{yy} and the electron g factor.[44] Two RSA traces measured at different temperatures are depicted in Figure 6(b). We note that the RSA signal shape changes drastically: for the measurement at 18 K, the total signal amplitude is significantly smaller (the signal has been multiplied by a factor of 17 to become comparable to the other trace), and the zero-and finite-field RSA peaks show a smaller difference in FWHM and amplitude than in the measurement taken at 26 K. Here, the zero-field maximum is so large that the finite-field maxima are hardly visible in the trace. It follows from the discussion of the RSA shape that T_{zz} drastically increases with the small temperature increase. We have performed a temperature-dependent measurement series in order to study this observation in more detail. The SDTs extracted from the RSA curves of this series are given in Figure 6(d) (note the log. scale for the SDT values). We clearly see that while the in-plane SDT, T_{yy}, remains almost unchanged at a value of a few ns in the temperature range investigated here, the out-of-plane SDT, T_{zz}, increases by an order of magnitude from less than 10 ns to more than 90 ns, with a maximum at 26 K. This value for the spin dephasing time significantly exceeds the largest results reported previously[45] for 110-grown 2DES. We can explain these observations as follows: at low temperatures, the remote dopant layers of the 2DES are not fully ionized. Therefore, on the one hand, the carrier concentration in the 2DES is increasing with temperature. This increase of the carrier concentration with temperature is also observed in photoluminescence spectra (not shown). On the other hand, the partial ionization leads to an asymmetry in the growth-axis band profile, which in turn induces a Rashba-type spin-orbit field. Since the orientation of this Rashba field is in-plane, DP-type spin dephasing of out-of-plane-oriented electron spins occurs, limiting the value of T_{zz} to a few nanoseconds. With increasing temperature, all the dopants in the remote doping layers are ionized, increasing the carrier density and drastically reducing the growth-axis asymmetry, thereby reducing the effective Rashba field. The DP-type spin dephasing for out-of plane spins is suppressed, yielding a drastic increase of T_{zz}. The upper limit for its value is given by the remaining Rashba fields, which may be due to a slight global asymmetry in the dopant layers, or due to fluctuations of the dopant concentration.[46] The fact that the *in-plane* SDT, T_{yy}, remains almost constant with temperature may also be explained by the changing carrier concentration: the in-plane spin dephasing is mostly driven by the Dresselhaus SOI, so that small changes of the Rashba field with temperature do not play a role. With increasing temperature, the carrier concentration, and therefore the Fermi energy and the amplitude of the Dresselhaus field at the Fermi wave vector increases. However, this increase is balanced by a reduction of the momentum scattering time with temperature, so that the spin dephasing rate remains nearly constant.

5. CONCLUSION

In conclusion, we have studied spin dynamics in two-dimensional electron and hole systems using time-resolved Faraday/Kerr rotation and resonant spin amplification techniques. While the mechanisms for spin dephasing for electrons and holes are very different, we observe very long spin dephasing times in excess of 80 ns for both types of carriers under certain experimental conditions. For holes, we identify two different initialization mechanisms for transfer of spin polarization from optically oriented to resident carriers. We demonstrate the advantages of resonant spin amplification versus time-resolved Kerr rotation concerning the measurement of long spin dephasing times in small magnetic fields. The combined spin and carrier dynamics are simulated using a coupled rate equation model, which yields excellent agreement to the experimental data. For electrons in a

(110)-grown two-dimensional electron system, we observe a large anisotropy between the out-of-plane and the in-plane SDTs, which reflects the symmetry of the spin-orbit fields in our sample.

ACKNOWLEDGMENTS

E. Sherman was supported by the MICINN of Spain grant FIS 2009-12773-C02-01, "Grupos Consolidados UPV/EHU del Gobierno Vasco" grant IT-472-10, and by the UPV/EHU program UFI 11/55. Partial support by a Research Group Linkage Project of the Alexander von Humboldt Foundation (P. Machnikowski and T. Kuhn) is gratefully acknowledged, as well as financial support by the DFG via GRK 1570, SFB689 and SPP1285.

REFERENCES

[1] Awschalom, D., Loss, D., and Samarth, N., [*Semiconductor Spintronics and Quantum Computation*], Springer (2002).

[2] Zutic, I., Fabian, J., and Das Sarma, S., "Spintronics: Fundamentals and applications," *Rev. Mod. Phys.* **76**, 323 (2004).

[3] Fabian, J., Matos-Abiague, A., Ertler, C., Stano, P., and Zutic, I., "Semiconductor Spintronics," *Acta Physica Slovaca* **57**, 565 (2007).

[4] Dyakonov, M. I., ed., [*Spin Physics in Semiconductors*], Springer,Berlin (2008).

[5] Wu., M. W., Jiang, J. H., and Weng, M. Q., "Spin dynamics in semiconductors," *Physics Reports* **493**, 61 (2010).

[6] Kikkawa, J. M. and Awschalom, D. D., "Resonant spin amplification in n-type GaAs," *Phys. Rev. Lett.* **80**, 4313 (May 1998).

[7] Kikkawa, J. and Awschalom, D., "Lateral drag of spin coherence in gallium arsenide," *Nature* **397**, 139 (1999).

[8] Kato, Y., Myers, R., Gossard, A., and Awschalom, D., "Coherent spin manipulation without magnetic fields in strained semiconductors," *Nature* **418**, 641 (2002).

[9] Crooker, S. A. and Smith, D. L., "Imaging spin flows in semiconductors subject to electric, magnetic, and strain fields," *Phys. Rev. Lett.* **94**, 236601 (2005).

[10] Crooker, S. A., Furis, M., Lou, X., Adelmann, C., Smith, D. L., Palmstrom, C. J., and Crowell, P. A., "Imaging Spin Transport in Lateral Ferromagnet/Semiconductor Structures," *Science* **309**, 2191 (2005).

[11] Karimov, O. Z., John, G. H., Harley, R. T., Lau, W. H., Flatte, M. E., Henini, M., and Airey, R., "High temperature gate control of quantum well spin memory," *Phys. Rev. Lett.* **91**, 246601 (2003).

[12] Malinowski, A., Britton, R. S., Grevatt, T., Harley, R. T., Ritchie, D. A., and Simmons, M. Y., "Spin relaxation in GaAs/$Al_xGa_{1-x}As$ quantum wells," *Phys. Rev. B* **62**, 13034 (2000).

[13] Brand, M. A., Malinowski, A., Karimov, O. Z., Marsden, P. A., Harley, R. T., Shields, A. J., Sanvitto, D., Ritchie, D. A., and Simmons, M. Y., "Precession and motional slowing of spin evolution in a high mobility two-dimensional electron gas," *Phys. Rev. Lett.* **89**, 236601 (2002).

[14] Dyakonov, M. I. and Perel, V. I., "Spin orientation of electrons associated with interband absorption of light in semiconductors," *Zh. Eksp. Teor. Fiz* **60**, 1954 (1971). [Sov. Phys. – JETP **33**, 1053 (1971)].

[15] Dyakonov, M. I. and Kachorovskiĭ, V. Y., "Spin relaxation of two-dimensional electrons in noncentrosymmetric semiconductors," *Soviet Physics - Semiconductors* **20**, 110 (1986).

[16] Ohno, Y., Terauchi, R., Adachi, T., Matsukura, F., and Ohno, H., "Spin relaxation in GaAs(110) quantum wells," *Phys. Rev. Lett.* **83**(20), 4196 (1999).

[17] Döhrmann, S., Hägele, D., Rudolph, J., Bichler, M., Schuh, D., and Oestreich, M., "Anomalous spin dephasing in (110) GaAs quantum wells: Anisotropy and intersubband effects," *Phys. Rev. Lett.* **93**, 147405 (2004).

[18] Hilton, D. J. and Tang, C. L., "Optical orientation and femtosecond relaxation of spin-polarized holes in GaAs," *Phys. Rev. Lett.* **89**, 146601 (2002).

[19] Baylac, B., Amand, T., Marie, X., Dareys, B., Brousseau, M., Bacquet, G., and Thierry-Mieg, V., "Hole spin relaxation in n-modulation doped quantum wells," *Solid State Communications* **93**, 57 (1995).

[20] Marie, X., Amand, T., Le Jeune, P., Paillard, M., Renucci, P., Golub, L. E., Dymnikov, V. D., and Ivchenko, E. L., "Hole spin quantum beats in quantum-well structures," *Phys. Rev. B* **60**(8), 5811 (1999).

[21] Syperek, M., Yakovlev, D. R., Greilich, A., Misiewicz, J., Bayer, M., Reuter, D., and Wieck, A. D., "Spin coherence of holes in GaAs/(Al,Ga)As quantum wells," *Phys. Rev. Lett.* **99**, 187401 (2007).

[22] Kugler, M., Andlauer, T., Korn, T., Wagner, A., Fehringer, S., Schulz, R., Kubová, M., Gerl, C., Schuh, D., Wegscheider, W., Vogl, P., and Schüller, C., "Gate control of low-temperature spin dynamics in two-dimensional hole systems," *Phys. Rev. B* **80**, 035325 (2009).

[23] Korn, T., Kugler, M., Griesbeck, M., Schulz, R., Wagner, A., Hirmer, M., Gerl, C., Schuh, D., Wegscheider, W., and Schüller, C., "Engineering ultralong spin coherence in two-dimensional hole systems at low temperatures," *New J. Phys.* **12**, 043003 (2010).

[24] Korn, T., "Time-resolved studies of electron and hole spin dynamics in modulation-doped GaAs/AlGaAs quantum wells," *Physics Reports* **494**, 415 (2010).

[25] Studer, M., Hirmer, M., Schuh, D., Wegscheider, W., Ensslin, K., and Salis, G., "Optical polarization of localized hole spins in p-doped quantum wells," *Phys. Rev. B* **84**, 085328 (2011).

[26] Heiss, D., Schaeck, S., Huebl, H., Bichler, M., Abstreiter, G., Finley, J. J., Bulaev, D. V., and Loss, D., "Observation of extremely slow hole spin relaxation in self-assembled quantum dots," *Phys. Rev. B* **76**, 241306 (2007).

[27] Baumberg, J. J., Awschalom, D. D., Samarth, N., Luo, H., and Furdyna, J. K., "Spin beats and dynamical magnetization in quantum structures," *Phys. Rev. Lett.* **72**, 717 (1994).

[28] Astakhov, G. V., Glazov, M. M., Yakovlev, D. R., Zhukov, E. A., Ossau, W., Molenkamp, L. W., and Bayer, M., "Time-resolved and continuous-wave optical spin pumping of semiconductor quantum wells," *Semicond. Sc. and Techn.* **23**(11), 114001 (2008).

[29] Yugova, I. A., Sokolova, A. A., Yakovlev, D. R., Greilich, A., Reuter, D., Wieck, A. D., and Bayer, M., "Long-term hole spin memory in the resonantly amplified spin coherence of InGaAs/GaAs quantum well electrons," *Phys. Rev. Lett.* **102**, 167402 (2009).

[30] Umansky, V., Heiblum, M., Levinson, Y., Smet, J., Nübler, J., and Dolev, M., "MBE growth of ultra-low disorder 2DEG with mobility exceeding $35{\times}10^6 \mathrm{cm}^2/\mathrm{Vs}$," *J. Crystal Growth* **311**, 1658 (2009).

[31] Rössler, C., Feil, T., Mensch, P., Ihn, T., Ensslin, K., Schuh, D., and Wegscheider, W., "Gating of high-mobility two-dimensional electron gases in GaAs/AlGaAs heterostructures," *New J. Phys.* **12**, 043007 (2010).

[32] Griesbeck, M., Glazov, M. M., Korn, T., Sherman, E. Y., Waller, D., Reichl, C., Schuh, D., Wegscheider, W., and Schüller, C., "Cyclotron effect on coherent spin precession of two-dimensional electrons," *Phys. Rev. B* **80**(24), 241314 (2009).

[33] Machnikowski, P. and Kuhn, T., "Theory of the time-resolved Kerr rotation in ensembles of trapped holes in semiconductor nanostructures," *Phys. Rev. B* **81**(11), 115306 (2010).

[34] Yugova, I. A., Glazov, M. M., Ivchenko, E. L., and Efros, A. L., "Pump-probe Faraday rotation and ellipticity in an ensemble of singly charged quantum dots," *Phys. Rev. B* **80**, 104436 (2009).

[35] Snelling, M. J., Flinn, G. P., Plaut, A. S., Harley, R. T., Tropper, A. C., Eccleston, R., and Phillips, C. C., "Magnetic g factor of electrons in GaAs/$\mathrm{Al}_x\mathrm{Ga}_{1-x}$As quantum wells," *Phys. Rev. B* **44**, 11345 (1991).

[36] Yakovlev, D. R. and Bayer, M., [*Spin Physics in Semiconductors*], vol. 157 of *Springer Series in Solid-State Sciences*, ch. Coherent Spin Dynamics of carriers, Springer, Berlin (2008).

[37] Luo, J.-W., Bester, G., and Zunger, A., "Atomistic pseudopotential calculations of thickness-fluctuation GaAs quantum dots," *Phys. Rev. B* **79**, 125329 (2009).

[38] Khaetskii, A. V., Loss, D., and Glazman, L., "Electron spin decoherence in quantum dots due to interaction with nuclei," *Phys. Rev. Lett.* **88**, 186802 (2002).

[39] Eble, B., Testelin, C., Desfonds, P., Bernardot, F., Balocchi, A., Amand, T., Miard, A., Lemaître, A., Marie, X., and Chamarro, M., "Hole–nuclear spin interaction in quantum dots," *Phys. Rev. Lett.* **102**, 146601 (2009).

[40] Fischer, J., Coish, W. A., Bulaev, D. V., and Loss, D., "Spin decoherence of a heavy hole coupled to nuclear spins in a quantum dot," *Phys. Rev. B* **78**, 155329 (2008).

[41] Kugler, M., Korzekwa, K., Machnikowski, P., Gradl, C., Furthmeier, S., Griesbeck, M., Hirmer, M., Schuh, D., Wegscheider, W., Kuhn, T., Schüller, C., and Korn, T., "Decoherence-assisted initialization of a resident hole spin polarization in a p-doped semiconductor quantum well," *Phys. Rev. B* **84**, 085327 (2011).

[42] Glazov, M. M. and Ivchenko, E. L., "Resonant spin amplification in nanostructures with anisotropic spin relaxation and spread of the electronic g factor," *Semiconductors* **42**, 951 (2008).

[43] Griesbeck, M., Glazov, M., Sherman, E., Korn, T., Schuh, D., Wegscheider, W., and Schller, C., "Anisotropic spin dephasing in a (110)-grown high-mobility GaAs/AlGaAs quantum well measured by resonant spin amplification technique," *Proceedings of SPIE* **8100**, 810015 (2011).

[44] Griesbeck, M., Glazov, M. M., Sherman, E. Y., Schuh, D., Wegscheider, W., Schüller, C., and Korn, T., "Strongly anisotropic spin relaxation revealed by resonant spin amplification in (110) GaAs quantum wells," *Phys. Rev. B* **85**, 085313 (2012).

[45] Müller, G. M., Römer, M., Schuh, D., Wegscheider, W., Hübner, J., and Oestreich, M., "Spin noise spectroscopy in GaAs (110) quantum wells: Access to intrinsic spin lifetimes and equilibrium electron dynamics," *Phys. Rev. Lett.* **101**, 206601 (2008).

[46] Sherman, E. Y., "Random spin-orbit coupling and spin relaxation in symmetric quantum wells," *Appl. Phys. Lett.* **82**, 209 (2003).